Complex Systems 1 (1987) 559–574

Lattice Models of the Lorentz Gas: Physical and Dynamical Properties

Philippe M. Binder
Center For Nonlinear Studies, Los Alamos National Laboratory, Los Alamos, NM 87545, USA
and
Applied Physics Section, Yale University, New Haven, CT 06520, USA

Abstract. This paper examines the validity and usefulness of cellular automaton models of fluid motion by means of a simple problem in kinetic theory.

We formulate three lattice models of the motion of a particle in a two-dimensional matrix of fixed, randomly placed, non-overlapping scatterers (the Lorentz gas). We measure several macroscopic and microscopic properties of this system, such as diffusion coefficients and mean-free paths. The results agree with analytical predictions, except at a high density of scatterers, where the models break down.

We also study these models as discrete dynamical systems. The properties of their state-transition diagrams, which give the number of all possible trajectories of the particle and their lengths, are similar to those of chaotic and random discrete maps. This agrees with analytical predictions that this gas exhibits chaotic behavior.

For this problem, we conclude that agreement between cellular automaton simulations and analytical results is very good.

1. Introduction

This paper studies the behavior of several cellular automaton models of the Lorentz gas. We present perhaps the most critical test to date for cellular automaton fluids. Since this is the simplest example of fluid motion with collisions, failure of the models to agree with analytical results would endanger the validity of cellular automaton simulations of fluids in general. Considering a simple problem in kinetic theory also offers several advantages: (a) there is a large body of analytical and computational results available, (b) we can easily study in detail microscopic properties of interest and not just average (macroscopic) properties, and (c) we can study in detail the gas as a discrete dynamical system and compare its properties with those of other discrete maps. For a system this simple, we can give a

complete description of the possible trajectories of the particle in terms of a state-transition diagram. To the best of our knowledge, this paper presents such a description of a discrete fluid mechanical system for the first time.

Both the physical properties and the dynamical system properties of the three models formulated in this paper agree well with analytical predictions. The physical properties studied in this paper are the dependence of the mean-free path on the density of scatterers, the long-time displacement distribution, and the dependence of the diffusion coefficient on the density of scatterers. The dynamical properties include the possible number of recurring trajectories (limit cycles) for a given configuration, the average length of a cycle, and the distribution of cycles starting from a randomly picked initial condition. Our results for these properties, in agreement with analytical predictions, indicate that the Lorentz gas exhibits chaotic behavior. We will now talk briefly about the lattice gas rules on which the models presented here are based.

Several models of fluid motion have been proposed [1–3] in which time is discrete and particles move and collide in a lattice. These models use collision rules which conserve mass, momentum, and energy at each node of the lattice; they belong to a class of discrete parallel-computing systems with local rules known as cellular automata. The macroscopic equations which result from some of these models [2,3] have been shown to approach the Navier-Stokes equation, which describes the motion of many incompressible fluids. Thanks to recent advances in parallel computation, it is possible that such models of fluid motion may soon compete with traditional computational methods.

Some effort has gone into testing these lattice gas models with standard problems of fluid mechanics such as shear flow and Poiseuille flow. The purpose of these tests has been to measure average quantities (e.g., velocity profiles or viscosities). Little effort has been made to follow microscopic motion in detail in these simulations. Also, since the number of possible states of the gas grows exponentially with the number of particles, a complete dynamical description of these many-particle problems is unfeasible.

This paper will proceed as follows. In section 2, we describe briefly the Lorentz model and several analytical results which will be of interest in the remainder of the paper. In section 3, we introduce the three new models for the Lorentz gas. These are simple modifications of the models presented for gases with collisions between moving particles in references 1 and 2. In section 4, we present the results for mean-free paths, displacement distributions, and diffusion coefficients, which mostly agree with analytical results. Section 5 has the results for the dynamical properties of the models; these will be discussed in light of similar results for random maps of integers and discrete versions of chaotic maps. Section 6 contains a summary and discussion of the results, most of which support the claim that cellular automaton models are useful in the simulation of gas dynamics.

2. The Lorentz gas

We study in this paper what is probably the simplest nontrivial example of fluid motion. The problem is the motion of a single particle embedded in a two-dimensional matrix or fixed, non-overlapping, randomly placed scatterers. It was first introduced by Lorentz [4] as a model of electronic motion in a solid. In his model, the particle represents a free electron and the scatterers represent atoms. He assumed the particle-scatterer collisions to be perfectly elastic.

Because of its simplicity, the Lorentz gas has been well studied and some of its properties have been derived mathematically [5–9]. There is disagreement between simulation and these analytical results for some quantities, especially the velocity autocorrelation function [10,11]. For the purposes of this paper, we will only study quantities for which this disagreement does not exist.

We are concerned with three physical properties of the Lorentz gas: the dependence of the mean-free path on the density of scatterers, the form of the displacement distribution, and the dependence of the diffusion coefficient on the density of scatterers.

The first property, the mean-free path, is the average distance traveled by the particle between collisions. If the positions of the scatterers are uncorrelated, the frequency of collisions should be proportional to the density of scatterers, and the mean-free path should be inversely proportional to the density. This is, indeed, the result given in section 10.5 of reference 7 for this gas. Reference 9 shows implicitly that the mean-free path and the density of particles are inversely proportional for an arbitrary lattice gas.

The second property is the long-time limit of the displacement distribution. This quantity is the average over scatterer configurations of the distance that the particle travels from a given point. Reference 5 shows that for long times this distribution obeys the central limit theorem, suggesting a Gaussian form.

The third property, the diffusion coefficient, is a macroscopic one. Its value is given by the time evolution of the mean-square displacement. The relevant analytical results are given in reference 8. In that paper, an expression for the diffusion coefficient is given to second order in the density of scatterers. This equation will be given in section 4. The authors do this for the wind-tree model, which is a Lorentz gas in which the particle (wind) is restricted to move in mutually perpendicular directions because of the placement of tilted square-shaped obstacles (trees).

3. Model

Three models were used to obtain the results reported in the next two sections; we will call them square lattice (S); triangular, time-alternating (TTA); and triangular, time-independent (TTI). These models have two common features: they are discrete in time and they are formulated in

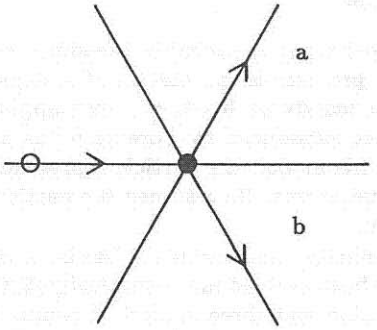

Figure 1: Collision rule for the triangular, time-alternating (TTA) model: upon hitting a scatterer, the particle has two possible trajectories: (a) at an odd time step, (b) at an even time step.

a regular plane-filling lattice (square or triangular). These models are straightforward adaptations of those in references 1 and 2, which show hydrodynamic behavior. For simplicity, we will take the edge length, time step, and velocity of the particle to be equal to one, so that all distributions, diffusion coefficients, and recurrence times come out dimensionless. Note that with this simplification, the mean-free time and the mean-free path are the same. In the first model, the particle moves between the nodes of a square grid at unit speed. The direction of the particle only changes when it hits a scatterer (randomly placed at the nodes of the grid). It does so by $\pm 90°$, according to the parity of the time step.

In the other two models, the particle moves in a triangular grid, so that at each node six directions—differing by angles of 60°—are possible. Unless a scatterer is present, the particle will go through a node without change in velocity. In the TTA case, the particle will undergo a $\pm 60°$ change in direction, according to the parity of the time step (see figure 1). Note that this case is the most similar to the FHP model for many particles, which approximates the Navier-Stokes equation [2]. For this reason, it will be the most carefully studied in this paper. In the TTI case, a scatterer will always cause a 60° deviation in the same direction, corresponding in every case to either only (a) or only (b) in figure 1.[1] So, after six collisions, a particle will have traveled in every possible direction. In this case, we can interpret the scatterers as point magnetic fields of just sufficient strength to make a charged particle change direction by exactly 60°. We have by now deviated considerably from the original problem, which contained only interactions between hard spheres.

In all models, we have used a parallelogram-shaped domain with helical

[1] A model similar to TTI but in a square lattice was introduced by M. Kac in D.J. Gates, *J. Math. Phys.*, **13** (1972) 1315.

boundary conditions, as introduced in reference 1. These boundary conditions are similar to periodic ones, except that the corresponding edges of the domain are slightly shifted. This was done to ensure that in the absence of scatterers the particle would sweep the entire space and show some semblance of ergodic behavior. The sole exceptions to these boundary conditions are the trajectories in figure 4, obtained with reflecting boundary conditions.

In order to study the effects of system size (more exactly, of number of states of the discrete system), we used lattices of size 64×64, 32×32, and 16×16 for all models. The trajectories in figure 4 were obtained in a 252×251 triangular lattice. We decided to study the case of nonoverlapping scatterers because it yields a nonzero diffusion coefficient [8]. The extension to overlapping scatterers could be done with collections of point scatterers.

The greatest disadvantages of these methods are that (a) the extension to three dimensions is still problematic [12] and (b) the change in behavior that we should expect for high density of scatterers does not occur. These obstacles, occupying no volume, do not restrict the motion of the particle as finite obstacles do. In particular, the diffusion coefficient does not go to zero in our models for high densities of scatterers.

These models are very different from the Lorentz lattice models for which Ernst and collaborators [10] calculated analytically the form of the velocity autocorrelation function and the diffusion coefficient. Their model consists of random walks on a square lattice with randomly excluded sites.

4. Physical properties

In this section, we describe the results that correspond to physically meaningful quantities for the Lorentz gas. These include the calculation of mean-free paths, long-time displacement distribution, and the diffusion coefficient.

4.1 Mean-free path

Figure 2 shows the average mean-free path versus the density of scatterers. The average was calculated over 400 different scatterer configurations with a random initial condition for the particle.[2] The mean-free path was calculated by dividing the recurrence time (number of time steps it takes the particle to return to its original position with its original velocity) by the number of collisions suffered during this time. Since the trajectory we used is reproduced endlessly in these models of the gas, we can consider

[2]Since the purpose of this paper is not to test the accuracy of a numerical method, we will not perform an exhaustive error analysis. We would like, however, to give the reader an idea of what it entails to pick only 400 configurations out of a large number of them—of the order of the possible number of arrangements of the scatterers on the lattice. We performed 20 runs each over 400 independent configurations of the 64×64 TTA lattice with 128 scatterers for the mean-free path and the diffusion coefficient. In the first case, the standard deviation was 0.7 percent and in the second it was 4.2 percent.

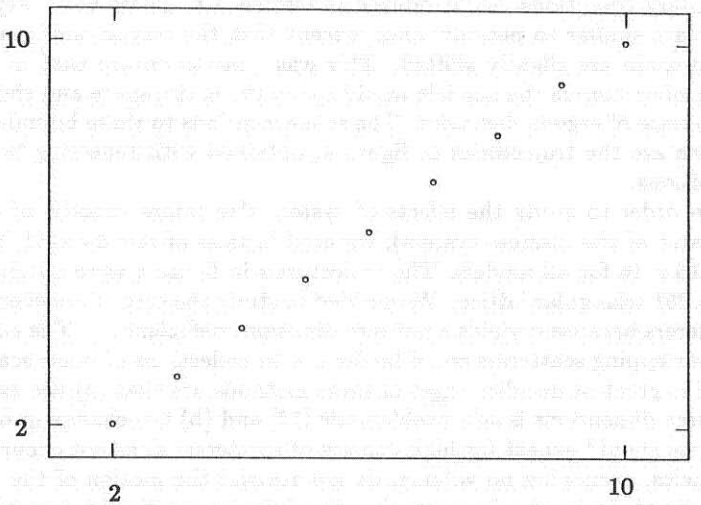

Figure 2: Average logarithm (base 2) of the mean-free path versus logarithm (base $\frac{1}{2}$) of the density of scatterers. This graph, obtained with a 64×64 TTA lattice, shows the inverse dependence of the mean-free path on the density of scatterers. Each point represents an average over 400 configurations of scatterers.

this result an infinite-time limit. The results for all three models are almost exactly the same; only the numbers for the 64×64 TTA lattice are shown. This figure shows that the mean free path is proportional to the inverse of the density of scatterers. This result is easily explained, since the probability of a collision is proportional to the number of scatterers present if their positions are uncorrelated. A derivation of this result is given in section 10.5 of reference 7. Reference 9 shows this result implicitly for lattice gases.

Figure 3 shows four complete trajectories of the TTA model (until recurrence occurs) in a 252×251 lattice, with reflecting boundary conditions. We will call these trajectories "cycles". This figure was obtained with a CAM-6 cellular automaton machine [13]. The six directions of motion, which appear to be 45° apart in the figure, are really multiples of 60° apart in the model. Figures 3a and c show very different mean-free path lengths, while 3b shows an almost ergodic trajectory and 3d one very constrained by scatterers. Figure 4 shows the distribution (over 400 cycles) of mean-free paths for the 64×64 TTA lattice with 1024 scatterers (average mean-free path $= 4.0$). This very narrow distribution is typical of all cases. There is a related result in section 5.4 of reference 7 that shows a narrow distribution for the mean-free path in a hard-sphere gas.

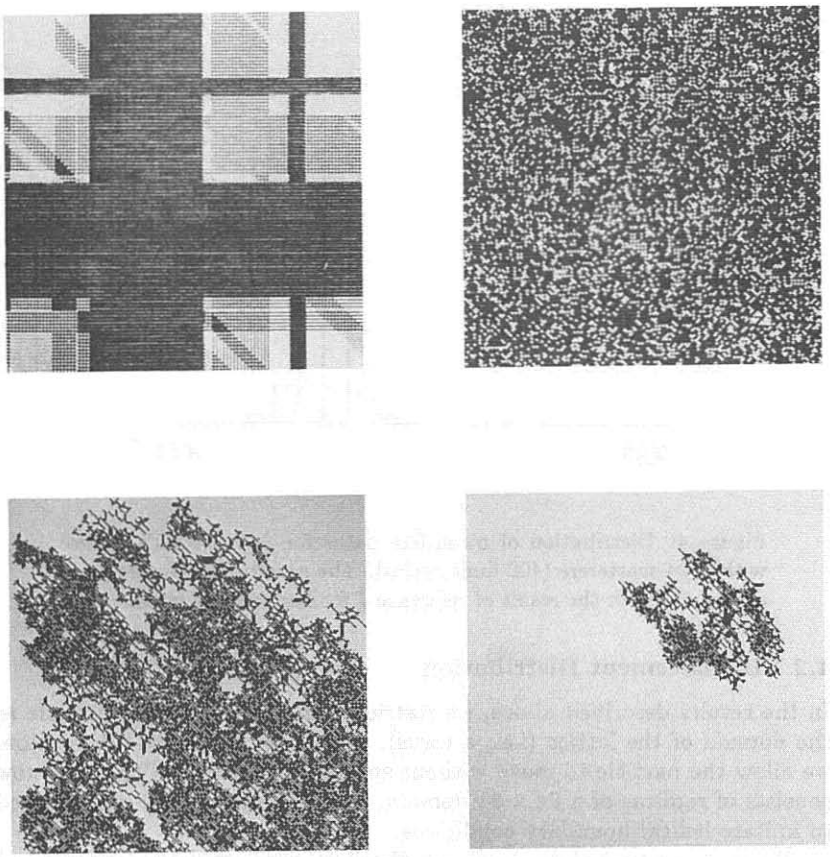

Figure 3: Recurring trajectories in a 252×251 TTA lattice with reflecting boundary conditions: (a) six scatterers (length: 81052), (b) 10 percent scatterers (length: 161350), (c) 25 percent scatterers (length: 85089); (d) 30 percent scatterers (length: 4913). Figure (a) shows a long mean-free path; (c) and (d) show short ones. Figure (b) shows ergodic behavior and (d) a very short cycle, constrained by the scatterers.

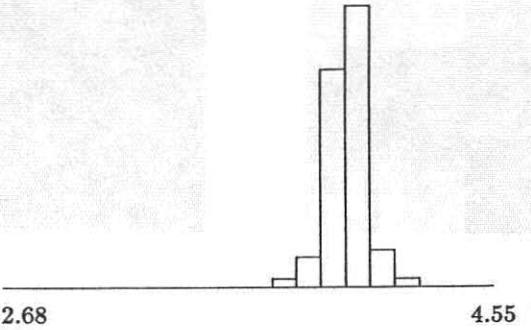

Figure 4: Distribution of mean-free paths for 64×64 TTA lattice with 1024 scatterers (400 limit cycles). The narrow distribution is in agreement with the result of reference 7 for hard-sphere gases.

4.2 Displacement Distribution

In the results described above, we restricted the motion of the particle to the domain of the lattice (i.e., a torus). In the remainder of this section, we allow the particle to move without spatial restrictions. The space now consists of replicas of a 64×64 domain, put together slightly mismatched to imitate helical boundary conditions.

Figure 5 is a typical displacement distribution (over 800 configurations) for long times, obtained with a 64×64 TTA lattice after 800 mean-free times. It is consistent with the central limit theorem results of reference 5. In other runs, we have observed that this form of distribution sets in after 80 to 100 mean-free times.

4.3 Diffusive Behavior

The calculation of the diffusion coefficient D given in this section uses the following definition of Einstein [14]:

$$\langle (r_x(t) - r_x(0))^2 \rangle \sim 2Dt. \tag{4.1}$$

Figure 6 shows a plot of the mean-square displacement (averaged over 200 scatterer configurations) versus time, which is linear in agreement with equation (4.1). This plot is for the 64×64 TTA lattice with 128 scatterers. The slope of this graph for long times gives the diffusion coefficient.

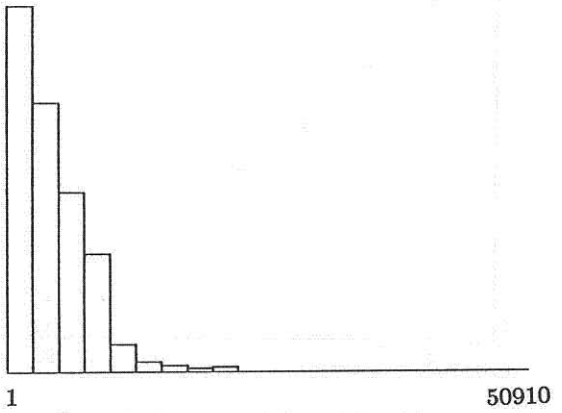

Figure 5: Long-time displacement distribution (800 mean-free times) for 64×64 TTA model with 64 scatterers. This result (which usually shows after about 100 mean-free times) agrees with the central-limit theorem results of reference 5.

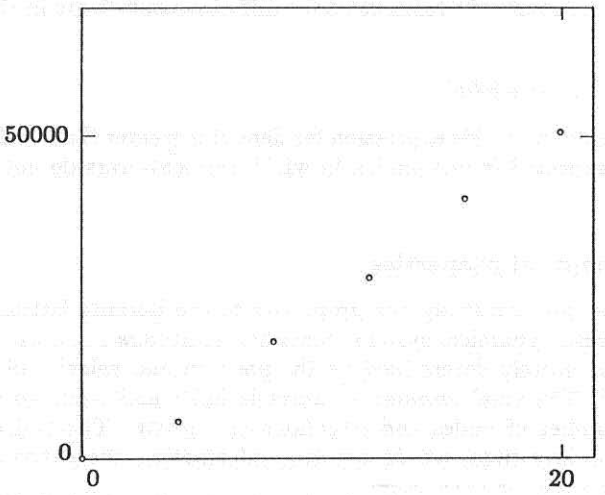

Figure 6: Mean-square displacement versus time (mean flights) for 64×64 TTA model with 128 scatterers. The slope of this graph gives the diffusion coefficient.

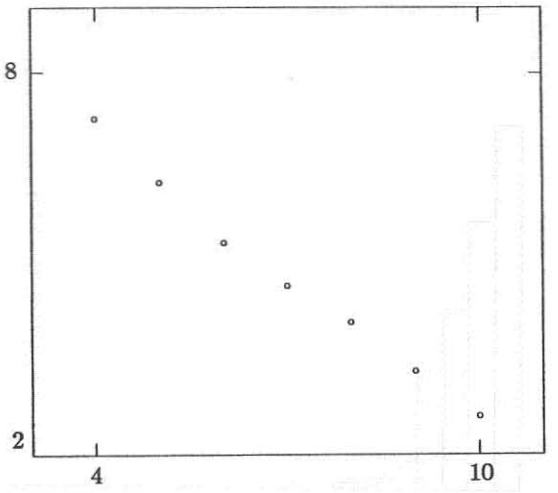

Figure 7: Natural logarithm of the dimensionless diffusion coefficient versus logarithm (base 2) of the density of scatterers. This result agrees with the prediction of reference 8 for the wind-tree model up to a density $\rho = \frac{1}{64}$.

In figure 7, we have plotted the diffusion coefficient versus density of scatterers. This plot appears to be linear, which agrees at low densities with the expression in reference 8 for diffusion coefficients in the wind-tree model,

$$D^{-1} \sim 2\rho + 6.5\rho^2 \tag{4.2}$$

but disagrees with this expression for densities greater than 0.01 or so. This is to be expected in our model, in which the scatterers do not occupy any area.

5. Dynamical properties

In this section, we study the properties of the Lorentz lattice gas viewed as a discrete dynamical system. Since the scatterers are fixed, the state of the gas is entirely determined by the position and velocity of the moving particle.[3] The total number of states is finite and equal to the product of the number of nodes and directions of velocity. The trajectory of the particle is invertible; we do not lose information about the state of the

[3]Strictly speaking, one must also give the parity of the time step in the time-alternating models, since the trajectory also depends on this parity. However, changing the parity of the initial time is equivalent to moving every scatterer a unit edge in the direction of motion; the result is another configuration, just as probable as the first. We can then ignore this additional complication as long as we are averaging over configurations. This will be the case for the first two of the three quantities reported in this section.

system at previous times. (All translation and collision steps have unique outcomes.) It follows that the evolution of the system will consist of one or several cycles, each of length equal to the time needed for the particle to return to its initial state. This is different from the behavior of discrete dissipative systems [15], in which transients are also present. The length of these cycles corresponds roughly to the first recurrence time in continuous aperiodic systems (see reference 16 for example). For a fixed number of scatterers, the average length of a cycle and the distribution of cycle lengths over all configurations of scatterers say all there is to be said about the gas as a discrete dynamical system. These are the results we will show next for the Lorentz gas.

Table 1 is a summary of average cycle lengths (expressed as a fraction of the total number of states of the system) for several models and lattice sizes. These were averaged over 400 scatterer configurations and initial conditions picked at random. Except for the case of one or two scatterers (not shown in the table), the average cycle length starting from an arbitrary initial condition appears to be one half of the total number of states. This result is independent of the model or system size.

One thing varies with the model: the distribution of cycle lengths for fixed number of scatterers averaged over randomly picked initial conditions. Figure 8 shows typical examples for the three models (all for 128 scatterers in a 64×64 lattice).

Figures 8a and b show this distribution for the S and TTA models; it is essentially uniform, but with a considerable peak for trajectories that visit most of the available states of the system. Figure 8c, the cycle length distribution for the TTI model, shows a uniform length distribution of cycles. An explanation for this difference is that since, in the TTI model, the particle travels in all six directions in the process of suffering six consecutive collisions, it is likely for a trajectory to curl around and recur faster than in the other models.

Table 2 shows results for the number of cycles in a given configuration for 16×16 and 32×32 TTI lattices; we have picked these to avoid the apparent doubling of phase space caused by the time-alternating rules. These results were averaged over 40 configurations each. The number of cycles increases with the density of scatterers; this density may play the same role as the nonlinearity parameter in a chaotic map. The expected number of cycles for a random mapping in systems of these sizes would be 7.3 and 8.7 cycles respectively.

We will now compare this state-transition description with the results for random maps of integers [17] and for the discrete standard map [18]. The standard map is a one-parameter, two-variable Hamiltonian map which can exhibit chaotic behavior. These results are the same in both cases, except that in the standard map they only apply for sufficiently high values of the nonlinearity parameter:

1. Starting from an initial condition picked at random, there is a uniform

Number of scatterers	Average fraction of phase space per cycle (randomly picked initial point)
64 × 64 TTA lattice (245776 states)	
4	0.47
16	0.57
64	0.55
256	0.53
512	0.54
32 × 32 TTA lattice (6144 states)	
4	0.48
16	0.54
64	0.52
256	0.54
16 × 16 TTA lattice (1536 states)	
8	0.50
16	0.54
32	0.52
64	0.54
64 × 64 S lattice (16384 states)	
16	0.48
64	0.48
256	0.54
1024	0.51
64 × 64 TTI lattice (24576 states)	
16	0.52
32	0.51
64	0.49
128	0.50

Table 1: Average of limit cycle lengths divided by total phase space for randomly picked initial configurations.

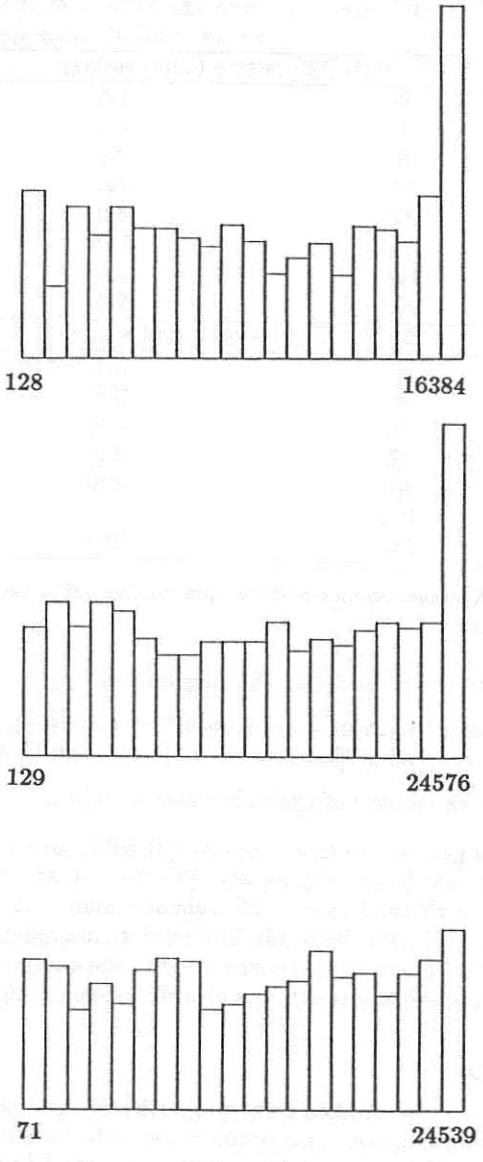

Figure 8: Distribution of limit cycle lengths starting from an arbitrary initial condition for 64×64 lattice with 128 scatterers: (a) S lattice; (b) TTA lattice; (c) TTI lattice. These distributions, especially the third one, agree with the predictions for random or chaotic maps. (400 randomly picked scatterer configurations and initial conditions).

Number of scatterers	Average number of cycles to cover all of phase space
16 × 16 TTI lattice (1536 states)	
2	1.8
4	2.9
8	2.7
16	3.0
32	3.9
64	5.55
128	9.0
200	9.5
32 × 32 TTI lattice (6144 states)	
4	2.5
8	2.8
16	3.2
32	3.8
64	4.8
128	6.4
256	12.2

Table 2: Average number of cycles per configuration versus number of scatterers.

probability distribution for the length of cycles.

2. The average length of a cycle that starts from an initial condition picked at random is $\frac{m}{2}$, where m is the total number of states.
3. The average number of cycles is equal to $ln(m)$.

For the Lorentz gas, we see that property (2) holds for all models, property (1) holds fairly well (especially for the TTI model), and property (3) is in fair agreement with the behavior of a chaotic map, and at high scatterer densities agrees well with the result for a random mapping. Although somewhat indirect, these results are consistent with the analytical and numerical results that the Lorentz gas exhibits chaotic behavior [19].

6. Summary

In this paper, we have studied some properties of three cellular automaton models of the Lorentz gas. This problem seems to have been overlooked in the simulations of lattice gases because it does not yield the Navier-Stokes equation, and because it does not take advantage of the parallelism inherent in these models.

It is essential, though, that good agreement exists between theory and lattice simulations for such a simple problem. We find such agreement in the physical and dynamical behavior of the lattice models presented in this paper.

We studied three physical properties of our models: (a) the dependence of mean-free path on the density of scatterers, which agrees with analytical results; (b) the long-time displacement distribution, which is consistent with analytical results; and (c) the diffusion coefficient. Although the time dependence of the mean-square displacement shows that this coefficient is well-defined, its dependence on density of scatterers disagrees somewhat with analytical results for a very similar model, the Ehrehfest wind-tree model. This is to be expected from the nature of our model, which does not restrict particle motion at high density of scatterers.

We also studied the state-transition graphs of the gas viewed as a discrete dynamical system; these graphs share to a large extent the properties of chaotic and random discrete maps for the distribution of limit cycles. Our results agree with the analytical prediction that the Lorentz gas exhibits chaotic behavior.

Some interesting work remains to be done, especially in the calculation of the Lyapunov exponent (to show explicitly chaotic behavior) and the computation of the velocity autocorrelation function, in which there is disagreement between theory and simulations.

In conclusion, the behavior of the lattice models of the Lorentz gas agrees well with that of their continuous counterpart, especially at low densities; this paper provides more evidence of the usefulness of cellular automata in simulating fluid mechanics.

Acknowledgements

Part of the work reported here was done during a visit to the Information Mechanics group at MIT; I thank its members, especially C. H. Bennett and N. Margolus, for their help and hospitality. I thank B. Atencio, Pierre Binder, L. M. de Bedout, and A. Moreno for their help with the figures, and G. Doolen, J. Erpenbeck, M. H. Ernst, J. D. Farmer, R. V. Jensen, and Y. C. Lee for their suggestions. This work was supported by the U. S. Department of Energy, Yale University, and the Air Force Office of Scientific Research (Grant AFOSR-ISSA-87-0095).

References

[1] J. Hardy, Y. Pomeau, and O. de Pazzis, *J. Math. Phys.*, **14** (1973) 1746; *Phys. Rev. A*, **13** (1976) 1949.

[2] U. Frisch, B. Hasslacher, and Y. Pomeau, *Phys. Rev. Lett.*, **56** (1986) 1505.

[3] S. Wolfram, *J. Stat. Phys.*, **45** (1986) 471.

[4] H. A. Lorentz, *Proc. Amst. Acad.*, **7** (1905) 438.

[5] L. A. Bunimovich and Ya. G. Sinai, *Commun. Math. Phys.*, **78** (1981) 479.

[6] J. M. J. van Leeuwen and A. Weijland, *Physica*, **36** (1967) 457; A. Weijland and J. M. J. van Leeuwen, *Physica*, **38** (1968) 35; M. H. Ernst and A. Weyland, *Phys. Lett. A*, **34** (1971) 39.

[7] S. Chapman and T. C. Cowling, *The Mathematical Theory of Nonuniform Gases* (Cambridge, 1970).

[8] E. H. Hauge and E. G. D. Cohen, *J. Math. Phys.*, **10** (1969) 397.

[9] M. Hénon, "Viscosity of a Lattice Gas", *Complex Systems*, **1** (1987) 760.

[10] T. M. Niewenhuizen, P. F. J. van Velthoven, and M. H. Ernst, *Phys. Rev. Lett.*, **57** (1986) 2477; M. H. Ernst, "Lorentz models revisited or what one can learn from ants in a labyrinth", in *Recent Developments in Nonequilibrium Thermodynamics: Fluids and Related Topics*, J. Casas-Vásquez, D. Jou, and J. M. Rubí, eds., *Lecture notes in Physics*, (Springer 1986) 253.

[11] B. J. Alder and W. E. Alley, *J. Stat. Phys.*, **19** (1978) 341; B. J. Alder and W. E. Alley, "The Lorentz gas", in *Perspectives in Statistical Physics*, ed. H. J. Raveché (North-Holland, 1981).

[12] D. d'Humières, P. Lallemand, and U. Frisch, *Europhys. Lett.*, **2** (1986) 291.

[13] T. Toffoli, *Physica D*, **10** (1984) 195.

[14] A. Einstein, *Ann. d. Physik*, **17** (1905) 549.

[15] T. Erber, T. Rynne, W. Darsow, and M. Frank, *J. Comput. Phys.*, **49** (1983) 394; P. M. Binder and R. V. Jensen, *Phys. Rev. A*, **34** (1986) 4460; C. Beck and G. Roepstorff, "Effects of phase space discretization on the long-time behavior of dynamical systems", RWTH Aachen preprint 1986 (*Physica D*, in press); H. Peck, tables 13 and 14 in "Theory and Applications of Cellular Automata", ed. S. Wolfram (World Scientific, 1986) 531–546.

[16] E. Fermi, J. Pasta, and S. Ulam, "Studies of nonlinear problems", document LA-1940, Los Alamos Scientific Laboratory (1955).

[17] M. Kruskal, *Am. Math. Monthly*, **61** (1954) 392; J. Riordan, *Ann. Math. Stat.*, **33** (1962) 178.

[18] F. Rannou, *Astron. and Astrophys.*, **31** (1974) 289.

[19] Ya. G. Sinai, *Sov. Math. Dokl.*, **4** (1963) 1818; J. P. Bouchaud and P. Le Doussal, *J. Stat. Phys.*, **41** (1985) 225.